

# Long time scale in Hamiltonian systems with internal degrees of freedom: Numerical study of a diatomic gas

Yoshihiro Watanabe<sup>1</sup>

*Department of Chemistry, Faculty of Sciences, Kyushu University  
Hakozaki, Fukuoka 812-8581, Japan*

Nobuko Fuchikami<sup>2</sup>

*Department of Physics, Tokyo Metropolitan University  
1-1, Minami-Ohsawa, Hachioji, Tokyo 192-0397, Japan*

---

## Abstract

We performed molecular dynamics simulations on a one-dimensional diatomic gas to investigate the possible long time scale inherent in heterogeneous Hamiltonian systems. The exponentially long time scale for energy sharing between the translational motion and the vibrational one certainly exists in a large limit of the system size. The time scale depends on the vibrational frequency  $\omega$  not as in the pure exponential form  $\sim \exp[B\omega]$  but as  $\sim \exp[B\omega^\alpha]$  with  $\alpha < 1$ , in good agreement with the expression derived from the Landau-Teller approximation. The numerical simulations show that the complete resonance condition for vibrational frequencies assumed in the analytical treatment is not essential for the long time scale. Some discussions of  $1/f$  fluctuations based on the present results will be given.

*Key words:* Slow dynamics, MD simulations, Boltzmann-Jeans conjecture, thermodynamic limit, heterogeneous systems,  $1/f^\alpha$  fluctuations.

*PACS:* 05.45.Pq, 05.40.Ca, 05.90.+m

---

## 1 Introduction

The experimental fact that the high frequency degrees of freedom do not contribute to the heat capacity of molecular gases is a seeming violation of the

---

<sup>1</sup> Email: yoshi@ccl.scc.kyushu-u.ac.jp

<sup>2</sup> Corresponding author. Email: fuchi@phys.metro-u.ac.jp

equipartition theorem in the classical statistical mechanics. As a possible explanation of this effective “freezing” phenomenon, Boltzmann[1] and Jeans [2] suggested more than one century ago that, if the time scale in vibration and the time scale associated with a typical binary collision in the gas are largely different, the amount of the energy exchanged between the vibrational and translational degrees of freedom can be small enough so that it takes an extremely long time for realization of thermal equilibrium. Although this problem was solved by the arrival of quantum mechanics, considerable attention has been paid to their original idea (the Boltzmann-Jeans conjecture) as a possible scenario of the slow dynamics in heterogeneous systems since their viewpoint was first noticed by Benettin et al. [3,4,5]. For example, a modified Fermi-Pasta-Ulam model which is composed of two subsystems with different time scales (corresponding to acoustic and optical vibrational modes) was analyzed to derive nonequipartition of energy in macroscopic systems [6].  $1/f$ -type energy fluctuations observed in molecular dynamics (MD) simulations of liquid water [7] and the long-term energy storage in protein molecules [8] were also discussed in the light of the Boltzmann-Jeans conjecture [9,10].

Generic nearly-integrable Hamiltonian systems have the stability time of the form

$$\tau_N \sim \exp[1/\varepsilon^\alpha] \quad \text{for } 0 < \varepsilon < \varepsilon_0 \quad (\text{the Nekhoroshev theorem}), \quad (1)$$

where  $\varepsilon$  is a positive parameter characterizing the smallness of the perturbation joined to an unperturbed integrable Hamiltonian;  $\alpha$  and  $\varepsilon_0$  are positive constants depending on the explicit form of the Hamiltonian, especially on the system size, i.e. the number  $N$  of degrees of freedom [11]. The time scale  $\tau_N$  grows exponentially as the perturbation parameter  $\varepsilon$  becomes small.

Equation (1) explains the non-ergodic behavior discovered in weakly coupled harmonic oscillators by Fermi, Pasta and Ulam (FPU phenomenon) for finite  $N$  [12]. However, the general proof based on the perturbational techniques yields a strong  $N$ -dependence for the constants:  $\alpha \sim 1/N$  and  $\varepsilon_0 \sim N^{-N}$  in the limit of  $N \rightarrow \infty$  [13], which implies that the FPU phenomenon will disappear in large systems or in the thermodynamic limit, although, as pointed out in [13], this general results do not exclude the possibility that some specified system of the FPU-type could actually exhibit the non-ergodic behavior in the large  $N$  limit [26].

Another type of Hamiltonian systems which can exhibit the long time scale of the Nekhoroshev-type is presented in refs. [4,5], the idea being based on the Boltzmann-Jeans conjecture. Such systems are represented by

$$H = H_0(p, q) + H_1(\pi, \xi) + f(p, q, \pi, \xi), \quad (2)$$

where  $H_0$  with the canonical variables  $p \equiv (p_1, \dots, p_\nu)$  and  $q \equiv (q_1, \dots, q_\nu)$  may generally be non-integrable in contrast to the unperturbed Hamiltonian in the Nekhoroshev theorem, while  $H_1$  describes the system composed of  $N$  harmonic oscillators:

$$H_1 = \sum_{i=1}^N \left( \frac{\pi_i^2}{2} + \frac{\omega_i^2 \xi_i^2}{2} \right) \quad (3)$$

with  $\pi \equiv (\pi_1, \dots, \pi_N)$  and  $\xi \equiv (\xi_1, \dots, \xi_N)$ . The interaction  $f$  is assumed to vanish for  $\xi = 0$ . The stability time is obtained as

$$\tau_B \sim \exp[(\lambda/\lambda^*)^\alpha], \quad (4)$$

where  $\lambda \equiv \omega/\Omega$  is the ratio of two typical time scales,  $1/\Omega$  in  $H_0$  and  $1/\omega$  in  $H_1$  and  $\lambda \gg 1$  is assumed. The positive constants  $\alpha$  and  $\lambda^*$  generally depend on the number  $N$  of harmonic oscillators.

When the angular frequencies  $(\omega_1, \dots, \omega_N)$  are nonresonant, the exponent  $\alpha$  is estimated again as  $\alpha \sim 1/N$ , but when  $\omega_1 = \dots = \omega_N \equiv \omega$  (the complete resonance) holds,  $\alpha = 1$  is proved for any  $N$ , so that the long time scale of the pure exponential form

$$\tau_B \sim e^{\lambda/\lambda^*} \equiv e^{B\omega} \quad (5)$$

is expected even for macroscopic systems as originally suggested by Jeans. If the stability time of the above form remains finite for  $N \rightarrow \infty$ , the basic idea of Boltzmann-Jeans could work as a key to reveal the dynamics of slow relaxation observed in macroscopic systems. The situation is, however, not so simple because the common perturbational techniques yield strong  $N$ -dependence of  $\lambda^*$  as  $\lambda^* \sim N^2$  even in the complete resonance case [16] and the long time scale cannot be guaranteed in the thermodynamic limit. Here too this does not mean the long time scale will always disappear for large systems. In fact, the above estimate of  $N$ -dependence seems to be statistically unacceptable if applied to sufficiently dilute molecular gases in which only binary collisions are relevant. Unfortunately, it is not easy to draw definite conclusions about the stability time (whether it remains finite or tends to zero in the thermodynamic limit) and its more reliable  $\omega$ -dependence (whether it is pure exponential or else) from direct simulations based on the molecular dynamics because the computational time steeply increases with the system size and the vibrational frequency, though such simulations were attempted for a diatomic gas nearly two decades ago [3].

Instead of invoking direct simulations, the  $\omega$ -dependence is considered from a different angle in [17]: By assuming a gas composed of identical diatomic

molecules (with  $\omega_1 = \dots = \omega_N = \omega$ ) and by applying the Landau-Teller approximation [18,19] to binary collisions between molecules the  $\omega$ -dependence of the time scale is obtained as

$$\sim \exp[B\omega^\alpha] \quad \text{with} \quad \alpha \equiv \frac{2}{3 + 2/s} < \frac{2}{3}, \quad (6)$$

where the inter-molecular potential  $\phi(r)$  is of the form

$$\phi(r) \sim \frac{1}{r^s}, \quad s \geq 1 \quad \text{for small } r. \quad (7)$$

In the present paper, we perform microcanonical MD simulations of a one-dimensional diatomic gas as a minimal model of macroscopic heterogeneous systems (i.e. systems with internal degrees of freedom) and investigate its long-term behavior to supplement with some information which has not been presented so far, hoping to find a clue to basic understanding of the slow relaxation phenomena observed in more realistic systems.

We first confirm whether the long time scale remains or not in the large  $N$  limit, which we think is necessary because the time scale does decrease with increasing  $N$  in a range of small  $N$  (for a fixed value of the number density). Next, we obtain its  $\omega$ -dependence to examine the Landau-Teller approximation. Since both the perturbation method leading to Eq. (5) and the Landau-Teller approximation applied to the binary collisions leading to Eq. (6) assume the condition of the complete resonance, we finally test the case in which  $(\omega_1, \dots, \omega_N)$  are slightly different with each other.

## 2 Hamiltonian and Initial Condition

We consider a one-dimensional molecular gas composed of  $N$  identical diatomic molecules with mass  $M$  [27]. The positions of two atoms belonging to the  $i$ th molecule are denoted by  $q_i - a - \xi_i$  and  $q_i + a + \xi_i$ , where  $q_i$  is the center of mass of the molecule and  $2a$  is the bond length,  $\pm\xi_i$  are the displacements of atoms from the equilibrium position. The total Hamiltonian is given by

$$H = N [K_{\text{tr}}(p) + K_{\text{vib}}(\pi) + V_{\text{vib}}(\xi) + V_{\text{int}}(q, \xi)], \quad (8)$$

where

$$K_{\text{tr}}(p) = \frac{1}{N} \sum_{i=1}^N \frac{p_i^2}{2M} \quad \text{with} \quad p_i \equiv M \frac{dq_i}{dt} \quad (9)$$

is the kinetic energy of translational motion of molecules,

$$K_{\text{vib}}(\pi) = \frac{1}{N} \sum_{i=1}^N \frac{\pi_i^2}{2M} \quad \text{with} \quad \pi_i \equiv M \frac{d\xi_i}{dt} \quad (10)$$

and

$$V_{\text{vib}}(\xi) = \frac{1}{N} \sum_{i=1}^N \frac{M\omega^2 \xi_i^2}{2} \quad (11)$$

are the kinetic and potential energies of intra-molecular vibrations, respectively, and

$$V_{\text{int}}(q, \xi) = \frac{1}{N} \sum_{i=1}^N \phi((q_i - a - \xi_i) - (q_{i-1} + a + \xi_{i-1})) \quad (12)$$

is the inter-molecular potential. We employ the cyclic boundary condition:  $q_0 \equiv q_N$  and  $\xi_0 \equiv \xi_N$ . The molecular interaction is identical with that adopted in [3], which is short range repulsive and given by

$$\phi(r) = \phi_0 \frac{e^{-(r/r_0)^2}}{r/r_0}, \quad r > 0. \quad (13)$$

In the present system,  $N [K_{\text{tr}}(p) + V_{\text{int}}(q, 0)]$  corresponds to  $H_0(p, q)$  with  $\nu = N$  and  $N [V_{\text{int}}(q, \xi) - V_{\text{int}}(q, 0)]$  to  $f(p, q, \pi, \xi)$  in Eq. (2). We may set  $M = r_0 = \phi_0 = 1$  without losing generality by choosing the units of mass, length and energy as  $M$ ,  $r_0$  and  $\phi_0$ , respectively. Then the unit of time is  $r_0 \sqrt{M/\phi_0} \equiv 2\pi/\Omega$ , which is a typical time scale characterizing the Hamiltonian  $H_0(p, q)$ . Note that  $\omega$  scaled by this time scale is actually read as the time scale *ratio*  $\omega/\Omega$  of the two subsystems.

Not like many FPU-type simulations starting from a state in which the energy is distributed to only specific normal modes, we chose a nearly thermal equilibrium state as the initial state, except in Section 3.5. This is because we are mainly interested in the long-term behavior observed in macroscopic systems in thermal equilibrium.

If the system represented by the Hamiltonian (8) is in a thermal equilibrium state with the temperature  $T$ , the expectation value of the kinetic energy  $K_{\text{tr}}$  (in the canonical ensemble) is calculated as

$$\langle K_{\text{tr}}(p) \rangle = \frac{\frac{1}{N} \sum_{i=1}^N \int \frac{p_i^2}{2M} e^{-H/kT} dq d\xi dp d\pi}{\int e^{-H/kT} dq d\xi dp d\pi}$$

$$= \frac{1}{N} \sum_{i=1}^N \frac{\int \frac{p_i^2}{2M} e^{-p_i^2/2MkT} dp_i}{\int e^{-p_i^2/2MkT} dp_i} = \frac{kT}{2}. \quad (14)$$

Note that Eq. (14) is exact even if the interaction term  $V_{\text{int}}(q, \xi)$  exists, because the variable  $p_i$  is separated from the rest of the variables. Similarly, one obtains

$$\langle K_{\text{vib}}(\pi) \rangle = \frac{kT}{2}, \quad (15)$$

which is also exact.

Without the term  $V_{\text{int}}$ , the Hamiltonian is decoupled into three terms with  $N$  degrees of freedom for each:  $NK_{\text{tr}}(p)$ ,  $NK_{\text{vib}}(\pi)$ , and  $NV_{\text{vib}}(\xi)$ ; and the expectation value of  $V_{\text{vib}}(\xi)$  in the thermal equilibrium state is also obtained rigorously as

$$\langle V_{\text{vib}}(\xi) \rangle = \frac{kT}{2}, \quad (16)$$

namely, the energy is equally distributed among three ‘‘subsystems’’ as

$$\langle NK_{\text{tr}}(p) \rangle = \langle NK_{\text{vib}}(\pi) \rangle = \langle NV_{\text{vib}}(\xi) \rangle = \frac{\langle H \rangle}{3}. \quad (17)$$

The present system is isolated (not contacted with the heat bath) and includes the coupling term  $V_{\text{int}}$ . However, if the coupling energy is relatively small and  $N$  is large, the energy of each subsystem in the stationary state is expected to be approximately equal, namely the long-time average for each subsystem satisfies

$$N\overline{K_{\text{tr}}(p)} \sim N\overline{K_{\text{vib}}(\pi)} \sim N\overline{V_{\text{vib}}(\xi)} \sim \frac{NE_{\text{tot}}}{3}, \quad (18)$$

where  $E_{\text{tot}}$  is the specific energy, i.e. the total energy of the system per molecule.

Taking account of the above, we start simulations with an initial state which is *approximately* thermal equilibrium as follows:

For the coordinate  $\xi$ , we generate  $N$  independent random numbers  $R_{\xi,i}$  ( $i = 1, 2, \dots, N$ ) with the normal distribution (Gaussian distribution with zero mean and unit variance) and set the initial value as  $\xi_i(0) = S_{\xi}R_{\xi,i}$ , where the positive constant  $S_{\xi}$  is chosen so that

$$V_{\text{vib},0} \equiv \frac{1}{N} \sum_{i=1}^N \frac{M\omega^2\xi_i(0)^2}{2} = \frac{E_{\text{tot}}}{3} \quad (19)$$

holds. This condition corresponds to Eq. (18), i.e. a thermal equilibrium state.

The initial position of the center of mass for each molecule is chosen as

$$q_i(0) = (i - 1)L + S_q R_{q,i}, \quad (20)$$

where  $L$  is the average molecular distance,  $S_q R_{q,i}$  is a small deviation from the average and  $R_{q,i}$  ( $i = 1, \dots, N$ ) are  $N$  independent random numbers with the normal distribution. The constant  $S_q$  is a small positive number so that the condition  $q_i(0) < q_{i+1}(0)$  ( $i = 1, \dots, N$ ) is satisfied. The initial value of the molecular interaction energy

$$V_{\text{int},0} \equiv V_{\text{int}}(q(0), \xi(0)) \quad (21)$$

is expected to be small by choosing the inter-molecular distance  $L$  being large enough in comparison to the potential parameter  $r_0$ .

Next, we choose the initial momentum  $p_i(0)$  ( $i = 1, \dots, N$ ) by a similar way as for  $\xi_i(0)$  but with a constraint  $\sum_{i=1}^N p_i(0) = 0$ : We generate  $N$  independent random numbers  $R_{p,i}$  with the normal distribution [28] and set  $p_i(0) = S_p (R_{p,i} - \sum_{j=1}^N R_{p,j}/N)$  with a constant  $S_p$  which satisfies

$$K_{\text{tr},0} \equiv \frac{1}{N} \sum_{i=1}^N \frac{p_i(0)^2}{2M} = \frac{E_{\text{tot}} - V_{\text{vib},0} - V_{\text{int},0}}{2}. \quad (22)$$

Then  $K_{\text{tr},0}$  is almost equal to  $E_{\text{tot}}/3$  when  $V_{\text{int},0}$  is small.

Finally  $\pi_i(0)$  ( $i = 1, 2, \dots, N$ ) are chosen from  $N$  independent random numbers  $R_{\pi,i}$  with normal distribution and set  $\pi_i(0) = S_\pi R_{\pi,i}$  with a constant  $S_\pi$  satisfying

$$K_{\text{vib},0} \equiv \frac{1}{N} \sum_{i=1}^N \frac{\pi_i(0)^2}{2M} = K_{\text{tr},0}. \quad (23)$$

Hereafter we mean the initial state satisfying Eqs. (19)  $\sim$  (23) by “nearly equilibrium initial state”. Since the parameters  $L$  and  $a$  appear only in the form  $L - 2a$  in  $V_{\text{int}}$  (see Eq. (12)), we may set  $a = 0$  by including its effect in the parameter  $L$ .

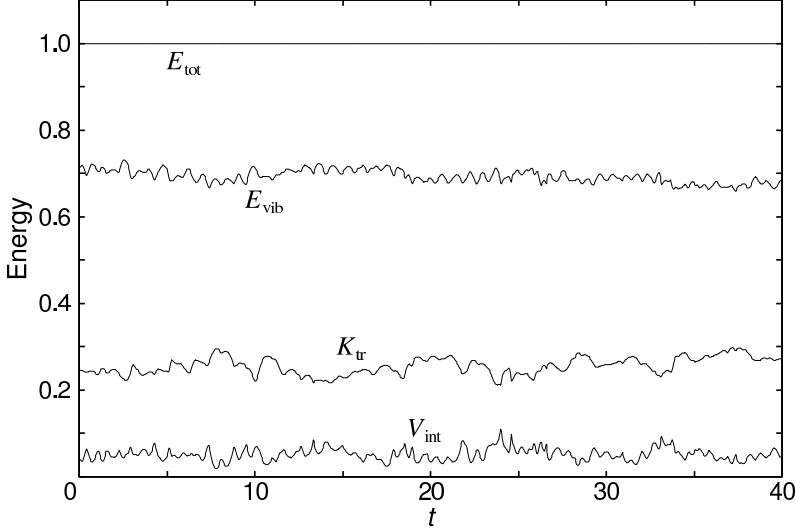


Fig. 1. A sample of the temporal fluctuations of energies for  $N = 128$  and  $\omega = 8$ .  $E_{\text{tot}}$ : the total energy (per molecule),  $K_{\text{tr}}$  the kinetic energy of the translational motion,  $E_{\text{vib}} = K_{\text{vib}} + V_{\text{vib}}$  the vibrational energy,  $V_{\text{int}}$  the molecular interaction energy. The initial condition:  $E_{\text{tot},0} = 1, V_{\text{vib},0} = 1/3, V_{\text{int},0} = 0.000\ 024, K_{\text{tr},0} = K_{\text{vib},0} = 0.333\ 322$ . Instantaneous values are plotted with the sampling time interval  $\Delta t = 0.04$  in the interval  $[230, 230 + 40]$  after the system was relaxed for  $t_{\text{relax}} = 230$ .

### 3 Numerical Results

The computer simulations were performed using the symplectic method [20]. As mentioned in the previous section, We set  $M = r_0 = \phi_0 = 1$ . Throughout the present simulations the average molecular distance was fixed as  $L = 4$ .

#### 3.1 Time evolution

Employing the initial condition in Eqs. (19) ~ (23), we started the simulation from a nearly thermal equilibrium state, in which  $K_{\text{tr}}(p) = K_{\text{vib}}(\pi) \approx V_{\text{vib}}(\xi) = E_{\text{tot}}/3$  and  $V_{\text{int}} \approx 0$ . The time dependence of energies of the total system (per molecule) for a short time interval  $230 \leq t \leq 230 + 40$  is presented in Fig. 1 for  $N = 128$  and  $\omega = 8$ , in which

$$E_{\text{tot}} \equiv K_{\text{tr}} + E_{\text{vib}} + V_{\text{int}} \quad (24)$$

and

$$E_{\text{vib}} \equiv K_{\text{vib}} + V_{\text{vib}}. \quad (25)$$

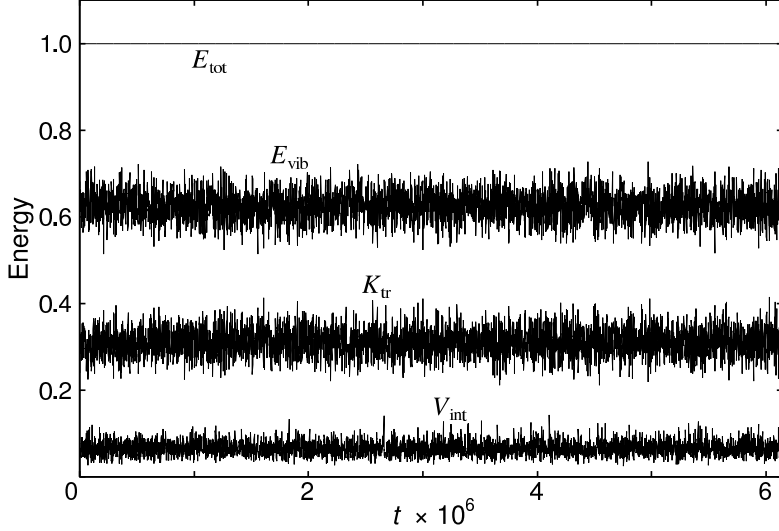


Fig. 2. Long time behavior. The same system parameters and the same initial condition as in Fig. 1. Instantaneous values are plotted at 4096 time points with the sampling interval  $\Delta t = 1500$ .

Figures 2, 3 and 4 show the long time behavior of energies and their standard deviations. In Fig. 3, the plotted point at the time  $t$  is the average of the quantity  $A$  defined by

$$\overline{A(t)} \equiv \frac{1}{t} \int_0^t A(t') dt'. \quad (26)$$

In Fig. 4, the standard deviation at the time  $t$  for the quantity  $A$  is plotted, which is defined by

$$\sigma(t) \equiv \sqrt{\overline{A(t)^2} - (\overline{A(t)})^2}. \quad (27)$$

Each energy and its standard deviation are plotted with the sampling time interval  $\Delta t = 1500$ . The final values of energies in Fig. 3 are  $E_{\text{tot}} = 1.000\,001\,63$ ,  $K_{\text{tr}} = 0.310\,09$ ,  $E_{\text{vib}} = 0.312\,39 + 0.311\,86 = 0.624\,25$ ,  $V_{\text{int}} = 0.065\,66$ . Those values agree well with the thermal equilibrium energies  $K_{\text{tr}} = (E_{\text{tot}} - V_{\text{int}})(N - 1)/(3N - 1) = 0.309\,82$ ,  $K_{\text{vib}} = V_{\text{vib}} = (E_{\text{tot}} - V_{\text{int}})N/(3N - 1) = 0.312\,26$  for  $N = 128$ . The factors  $(N - 1)/(3N - 1)$  and  $N/(3N - 1)$  instead of  $1/3$  appear because the center of mass of the total system is at rest. In Fig. 4, the final value of the standard deviation  $\sigma$  of the total energy  $E_{\text{tot}}$  is  $1.2 \times 10^{-5}$ , which is a measure of the computational error.

It should be noted that the energies of individual molecules change quite largely (compare with  $E_{\text{tot}} = 1$  which is averagely distributed to each molecule) as can be seen in Fig. 5 in which instantaneous energies of molecule 1 are plot-

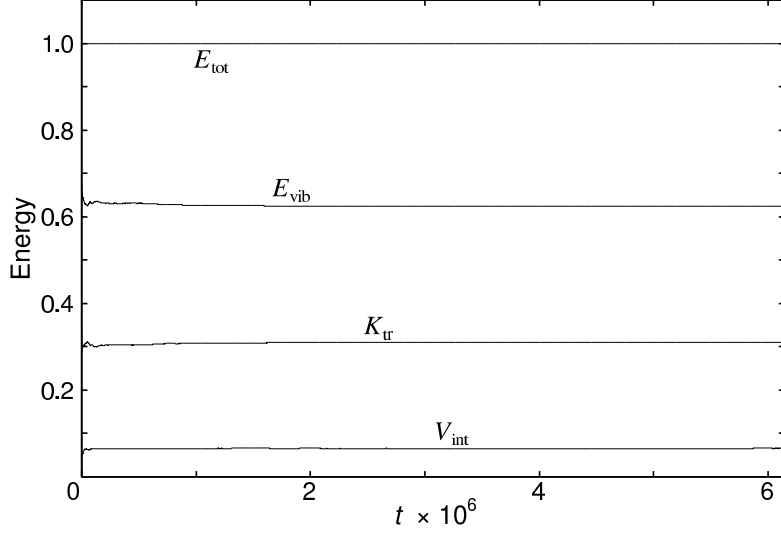


Fig. 3. Long time behavior of energy fluctuations. The same run as in Fig. 2, but the plotted point at the time  $t$  represents the average over the time interval  $[0, t]$  defined by (26). The sampling interval is the same as in Fig. 2.

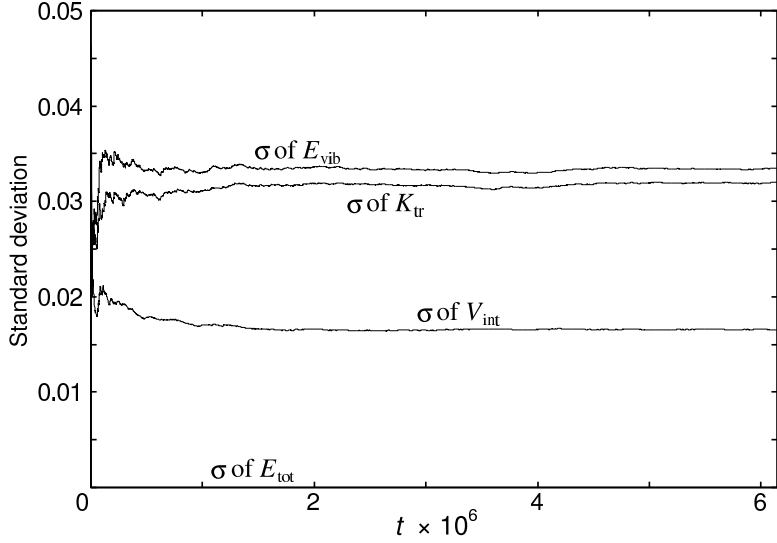


Fig. 4. Standard deviation  $\sigma$  of energies corresponding to Fig. 3. Plotted points at the time  $t$  are obtained from (27). The sampling interval is the same as in Fig. 2. The standard deviation of the total energy,  $\sigma$  of  $E_{\text{tot}}$ , is  $1.2 \times 10^{-5}$ .

ted. The large energy exchange is induced by the collision with the neighboring molecules as seen from Fig. 6.

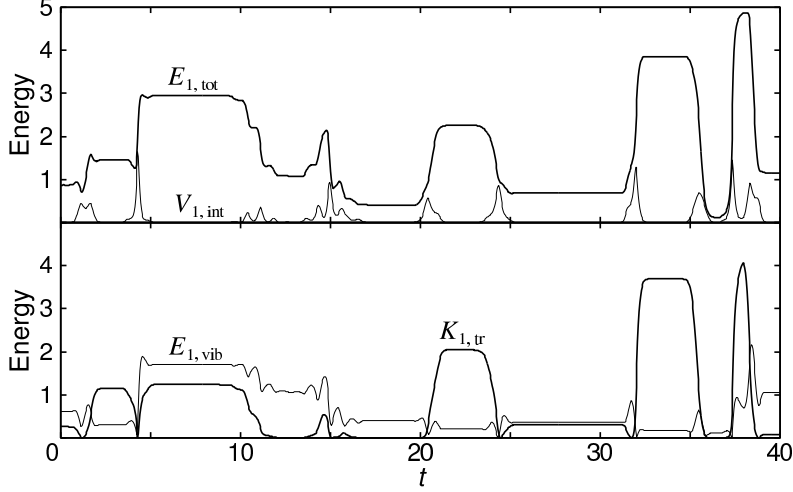


Fig. 5. Energies of molecule 1 in the same run as in Fig. 1.  $K_{1,\text{tr}} = p_1^2/2M$ ,  $E_{1,\text{vib}} = \pi_1^2/2M + M\omega^2\xi_1^2/2$ ,  $V_{1,\text{int}} = (\phi(q_1 - q_0 - \xi_1 - \xi_0) + \phi(q_2 - q_1 - \xi_2 - \xi_1))/2$ ,  $E_{1,\text{tot}} = K_{1,\text{tr}} + E_{1,\text{vib}} + V_{1,\text{int}}$ .

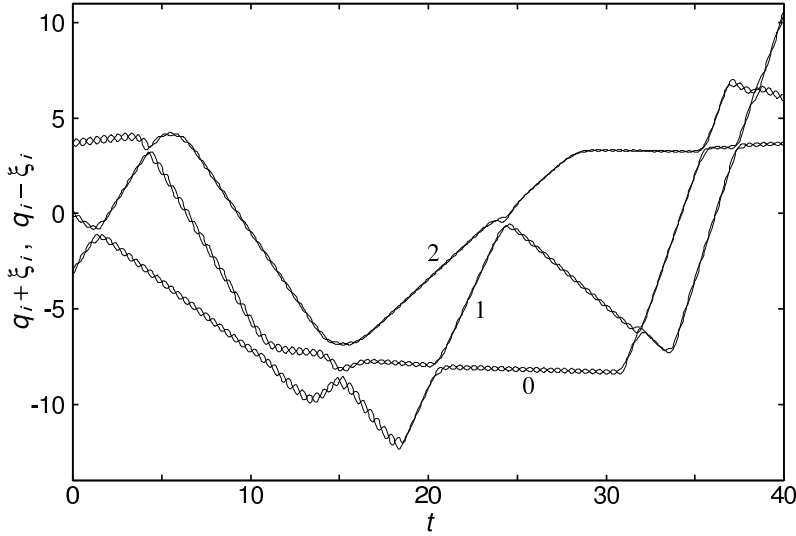


Fig. 6. Motion of atoms belonging to molecules 0, 1 and 2. The coordinates of atoms  $q_i \pm \xi_i$  ( $i = 0, 1, 2$ ) are plotted in the same run as in Fig. 1.

### 3.2 Size-dependence of the correlation time

As a time scale characterizing the system in equilibrium, one may employ the correlation time of the energy fluctuation. Following [3], we computed the correlation time  $\tau_{\text{cor}}$  of the vibrational energy  $E_{\text{vib}}$  which is defined such that the normalized correlation function

$$G(\tau) \equiv \frac{\overline{E_{\text{vib}}(t)E_{\text{vib}}(t+\tau)} - (\overline{E_{\text{vib}}(t)})^2}{\overline{E_{\text{vib}}(t)^2} - (\overline{E_{\text{vib}}(t)})^2} \quad (28)$$

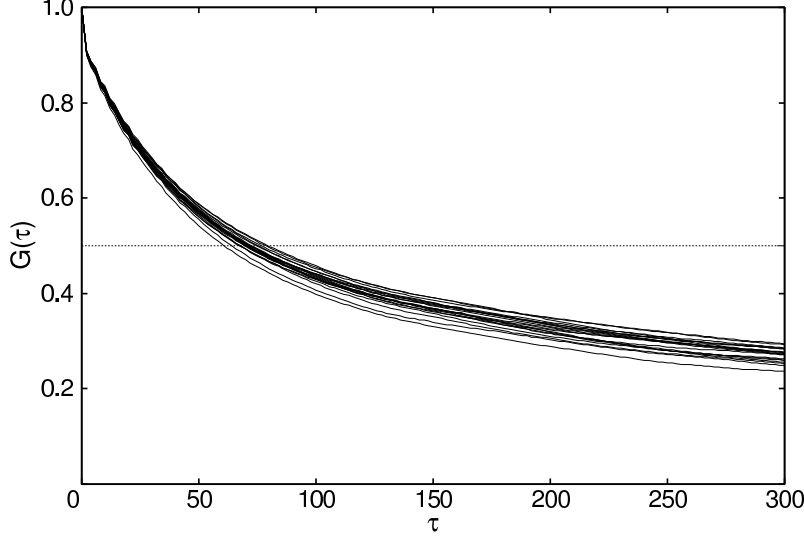


Fig. 7. Correlation function  $G(\tau)$  of the vibrational energy  $E_{\text{vib}}$  for 20 independent runs with nearly equilibrium initial states.  $N = 128$ ,  $\omega = 8$ ,  $E_{\text{tot}} = 1$ .

becomes a half of the initial value  $G(0) = 1$ :

$$G(\tau_{\text{cor}}) = 0.5, \quad (29)$$

where the overline denotes the time average over the dummy variable  $t$  for a sufficiently large interval  $t_{\text{obs}}$ .

We computed  $\tau_{\text{cor}}$  for various samples with different random initial conditions satisfying Eqs. (19)  $\sim$  (23) and define the average by

$$\bar{\tau}_{\text{cor}} \equiv \text{Ave} [\tau_{\text{cor}}]. \quad (30)$$

We have also employed another averaged correlation time  $\tau'_{\text{cor}}$  which is defined such that

$$\bar{G}(\tau'_{\text{cor}}) \equiv 0.5, \quad (31)$$

where  $\bar{G}(\tau)$  is the correlation function averaged over the samples:

$$\bar{G}(\tau) \equiv \text{Ave} [G(\tau)]. \quad (32)$$

The correlation time  $\tau'_{\text{cor}}$  is more easily estimated especially when  $G(\tau)$  decays very slowly in some samples and it takes very long time to obtain the average  $\bar{\tau}_{\text{cor}}$  over all samples, which actually occurs for small  $N$ .

The correlation function  $G(\tau)$  is plotted in Fig. 7 for  $N = 128$ ,  $\omega = 8$ ,  $E_{\text{tot}} = 1$  and for 20 samples with different random initial states satisfying (19)  $\sim$  (23).

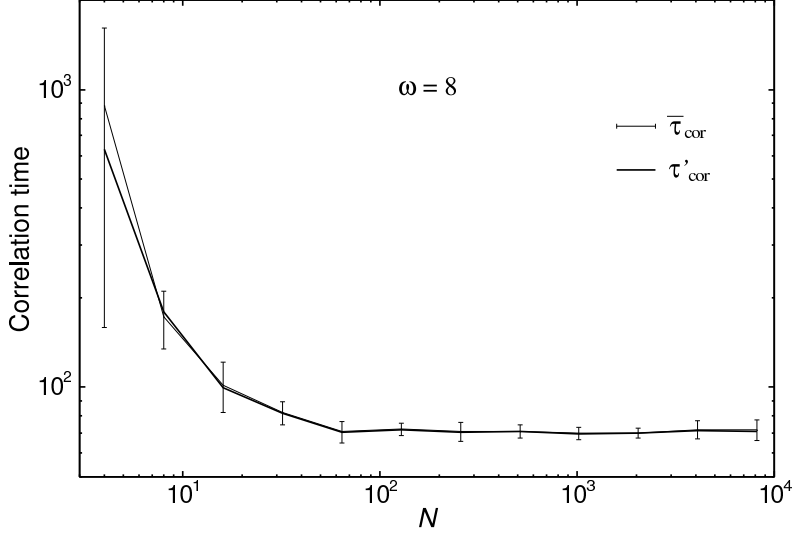


Fig. 8. System size dependence of the time scale. Two kinds of correlation time  $\bar{\tau}_{\text{cor}}$  defined by (30) and  $\tau'_{\text{cor}}$  by eq. (31) are plotted against the number  $N$  of molecules. The average is taken over 20 samples, i.e. 20 independent runs starting from nearly equilibrium initial states. The error bars indicate  $\bar{\tau}_{\text{cor}} \pm \sigma$ , where  $\sigma$  is the standard deviation for 20 samples.  $\omega = 8$ ,  $E_{\text{tot}} = 1.0$ .

To estimate  $G(\tau)$  reliably over the range  $0 \leq \tau \leq 300$ , the time average was taken in the interval  $[t_{\text{relax}}, t_{\text{relax}} + t_{\text{obs}}]$  with the observation time  $t_{\text{obs}} = 1 \times 10^6$  after the system was relaxed for  $t_{\text{relax}} = 2 \times 10^4$ .

In Fig. 8,  $\bar{\tau}_{\text{cor}}$  and  $\tau'_{\text{cor}}$  are plotted against the system size, i.e. the number  $N$  of molecules, from  $N = 4$  to  $N = 8192$ , where  $\omega = 8$  and the specific energy is fixed at  $E_{\text{tot}} = 1.0$ . The average is obtained from 20 independent runs starting from nearly equilibrium initial states and the error bars indicate  $\pm \sigma$ ,  $\sigma$  being the standard deviation of  $\tau_{\text{cor}}$  for 20 runs. The correlation time as a function of  $N$  decreases with increasing  $N$  in the beginning but tends to a finite value  $\approx 71$  as  $N \rightarrow \infty$ . The difference between  $\bar{\tau}_{\text{cor}}$  and  $\tau'_{\text{cor}}$  is large for small values of  $N$  but very small for large  $N$ . The error bar of  $\bar{\tau}_{\text{cor}}$  also becomes small for large  $N$  if the precision of the numerical simulation is high enough. Figure 8 proves that the correlation time certainly stays finite for large  $N$ , where the molecular density is fixed at  $1/L = 1/4$ .

We have obtained a similar size dependence for a larger value of the specific energy: When  $E_{\text{tot}} = 2.0$  with  $\omega = 8$ , both  $\bar{\tau}_{\text{cor}}$  and  $\tau'_{\text{cor}}$  tend to  $\approx 10.9$  with increasing  $N$  as  $(N, \bar{\tau}_{\text{cor}} \pm \sigma, \tau'_{\text{cor}}) = (8, 13.6 \pm 4.7, 13.0)$ ,  $(16, 11.0 \pm 1.0, 10.9)$ ,  $(32, 11.1 \pm 0.6, 11.0)$ ,  $(64, 11.0 \pm 0.3, 11.0)$ ,  $(128, 10.9 \pm 0.2, 11.0)$ ,  $(256, 10.9 \pm 0.1, 11.0)$ ,  $(512, 10.9 \pm 0.1, 10.9)$ . For larger values of  $E_{\text{tot}}$ , naturally the time scale is smaller but reaches a constant value faster. Similar dependence of the time scale on the system size and on the specific energy has been reported from the numerical simulations of FPU  $\beta$ -model [14].

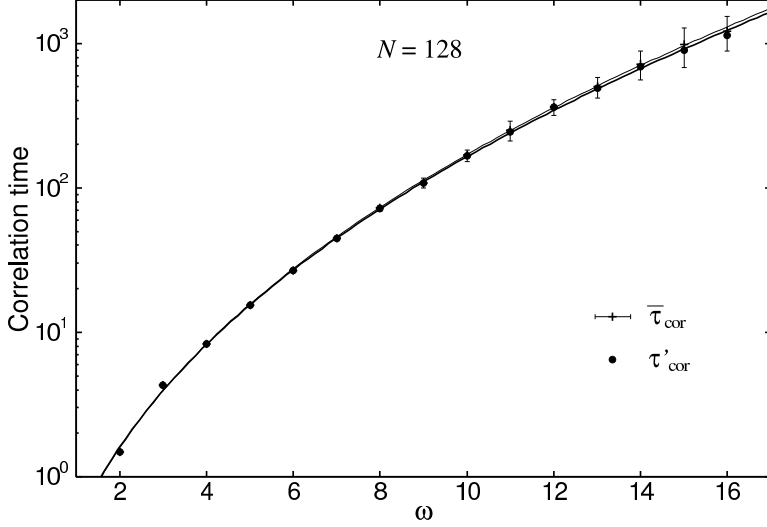


Fig.9

Fig. 9. Semilog plot of  $\omega$ -dependence of the averaged correlation times  $\bar{\tau}_{\text{cor}}$  and  $\tau'_{\text{cor}}$ . The average is taken over 20 independent runs. Error bars indicate  $\bar{\tau}_{\text{cor}} \pm \sigma$ , where  $\sigma$  is the standard deviation for 20 runs with nearly equilibrium initial states. The fitting lines are  $\bar{\tau}_{\text{cor}} = 0.0090 \times \exp[3.92 \times \omega^\alpha]$  and  $\tau'_{\text{cor}} = 0.0096 \times \exp[3.88 \times \omega^{0.4}]$  with  $\alpha = 0.4$ .  $N = 128, E_{\text{tot}} = 1.0$ .

### 3.3 $\omega$ -dependence of the correlation time

In Fig. 9, the averaged correlation times  $\bar{\tau}_{\text{cor}}$  and  $\tau'_{\text{cor}}$  are plotted against  $\omega$  for  $N = 128$ . If the mathematical theorem (5) is applied directly to the present system in which the condition  $\omega_1 = \dots = \omega_N = \omega$  is satisfied, the plot should drop on the straight line:  $\sim \exp[B\omega^\alpha]$ , with  $\alpha = 1$ , while the present results can be fitted better with  $\alpha$  smaller than one. The lines are for  $\alpha = 0.4$ , which was suggested from Eq. (6) (the Landau-Teller approximation) with  $s = 1$  corresponding to  $\lim_{r \rightarrow 0} \phi(r) \sim 1/r^s$  for the potential  $\phi(r)$  in Eq. (13). We obtained the fitting curves  $\bar{\tau}_{\text{cor}} = A \exp[B\omega^{0.4}]$  with  $(A, B) = (0.0090, 3.92)$  and  $\tau'_{\text{cor}} = A' \exp[B'\omega^{0.4}]$  with  $(A', B') = (0.0096, 3.88)$  [30]. Also, Fig. 10 shows good fitting to the same  $\omega$ -dependence in case of  $N = 256$  with  $(A, B) = (0.0096, 3.88)$  for  $\bar{\tau}_{\text{cor}}$  and  $(A', B') = (0.0102, 3.85)$  for  $\tau'_{\text{cor}}$ .

Deviation of the  $\omega$ -dependence from the pure exponential form can be qualitatively understood as follows [17]: The energy transfer  $\Delta E$  from the translational motion to the vibrational one arises dominantly from direct binary collisions of molecules. The two subsystems of translational and vibrational degrees of freedom are assumed to be in equilibrium states with well-defined temperatures  $T_{\text{tr}}$  and  $T_{\text{vib}}$ , respectively during the single binary collision. The Landau-Teller approximation applied to a single binary collision yields  $\Delta E$  as a function of the asymptotic data of two molecules before the collision, which is of the form  $\Delta E \sim e^{-\tau\omega}$ . The parameter  $\tau$  depends on the asymptotic value  $p$  (at  $t = -\infty$ ) of the relative momentum of the molecules, or equivalently

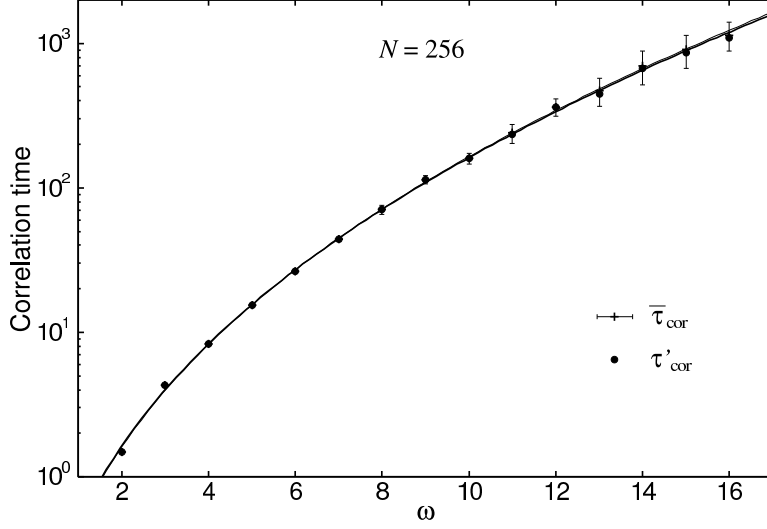


Fig.10

Fig. 10. The same as in Fig. 9 but for  $N = 256$ . The fitting lines are  $\bar{\tau}_{\text{cor}} = 0.0096 \times \exp[3.88 \times \omega^\alpha]$  and  $\tau'_{\text{cor}} = 0.102 \times \exp[3.85 \times \omega^\alpha]$  with  $\alpha = 0.4$ .

on the translational energy  $E_{\text{tr}} \sim p^2/2$ , and is expressed as  $\tau \sim (E_{\text{tr}})^{-\gamma}$  with  $\gamma = (s + 2)/2s > 0$  for the inter-molecular potential (7). The average energy exchange per unit time is given by integrating  $\Delta E$  over various asymptotic states with the Boltzmann factor  $\exp[-E_{\text{tr}}/kT_{\text{tr}} - E_{\text{vib}}/kT_{\text{vib}}]$ . Then the final form of the main  $\omega$ -dependence of the average energy exchange per unit time becomes stretched exponential:

$$\begin{aligned} \langle \Delta E \rangle &\sim \int_0^\infty \exp[-(E_{\text{tr}})^{-\gamma} \omega] \exp[-E_{\text{tr}}/kT_{\text{tr}}] dE_{\text{tr}} \\ &\sim \exp[-B\omega^\alpha] \end{aligned} \quad (33)$$

with

$$\alpha = 1 - \frac{\gamma}{1 + \gamma} = \frac{2}{3 + 2/s}, \quad (34)$$

which leads to the time scale  $\sim 1/\langle \Delta E \rangle$  as in Eq. (6). The origin of the exponent  $\alpha$  smaller than one arises from the balance of the negative exponent  $-\gamma$  in the parameter  $\tau$ , (i.e. the energy exchange  $\Delta E \sim e^{-\tau\omega}$  in individual collisions increasing with  $E_{\text{tr}}$ ) and the weight of the Boltzmann factor decreasing with  $E_{\text{tr}}$ .

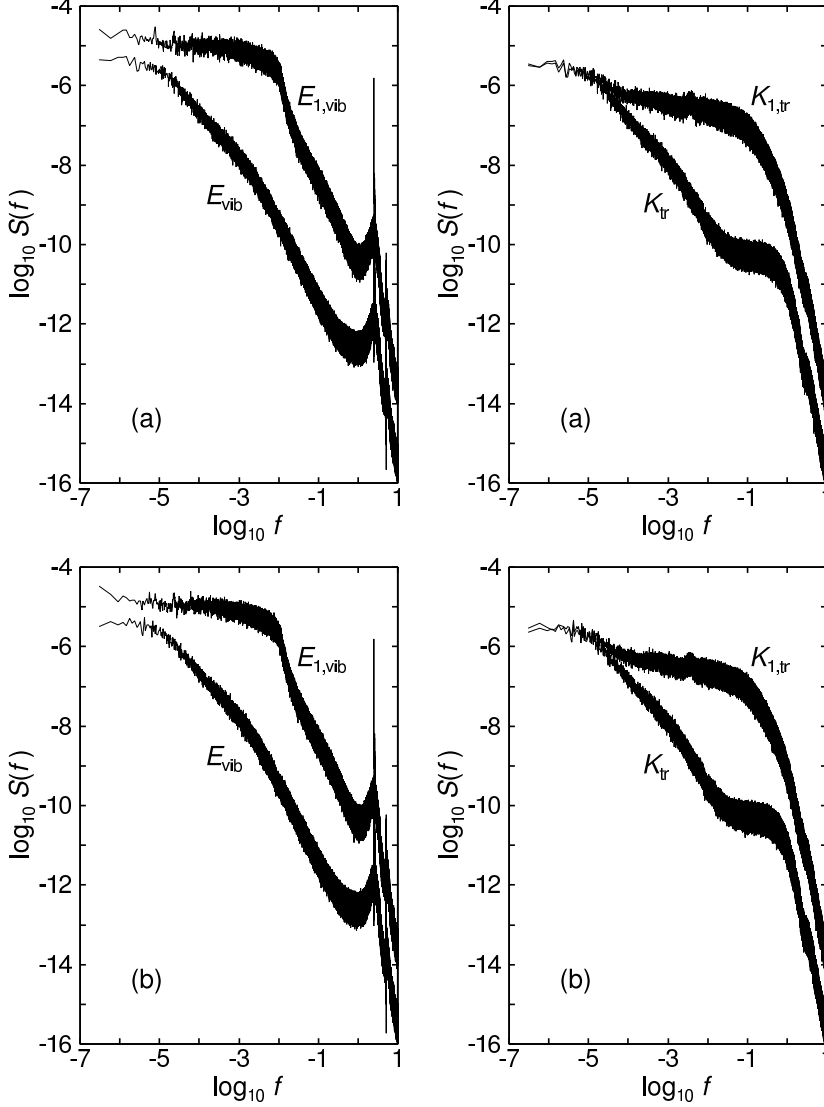


Fig. 11. (a) Log-log plot of PSD for the vibrational energy:  $E_{\text{vib}}$  and for translational energy:  $K_{\text{tr}}$ . The spectra for energies of a single molecule are denoted by  $E_{1,\text{vib}}$  and  $K_{1,\text{tr}}$ .  $N = 128$ ,  $\omega = 16$ ,  $E_{\text{tot}} = 1.0$ . The time interval of FFT time series data is  $\Delta t = 0.05$ , the number of the FFT data is  $N_{\text{dat}} = 2^{26}$ , i.e. the observation time is  $t_{\text{obs}} = 3.4 \times 10^6$ . Each PSD was obtained from the average over 20 independent runs with nearly equilibrium initial states. (b) The same as in (a) but with the initial states which are the final states of 20 runs in (a).

### 3.4 Power spectra and various time scales

The power spectrum density (PSD)  $S(f)$  of energy fluctuations is presented in Fig. 11(a) for vibrational motion and for translational one, where  $\omega = 16$ ,  $N = 128$ ,  $E_{\text{tot}} = 1.0$  and the observation time  $t_{\text{obs}} = 3.4 \times 10^6$ . The sharp peak at  $f_{\text{vib}} \equiv \omega/2\pi \approx 2.5$  in the spectrum of  $E_{\text{vib}}$  corresponds to the smallest

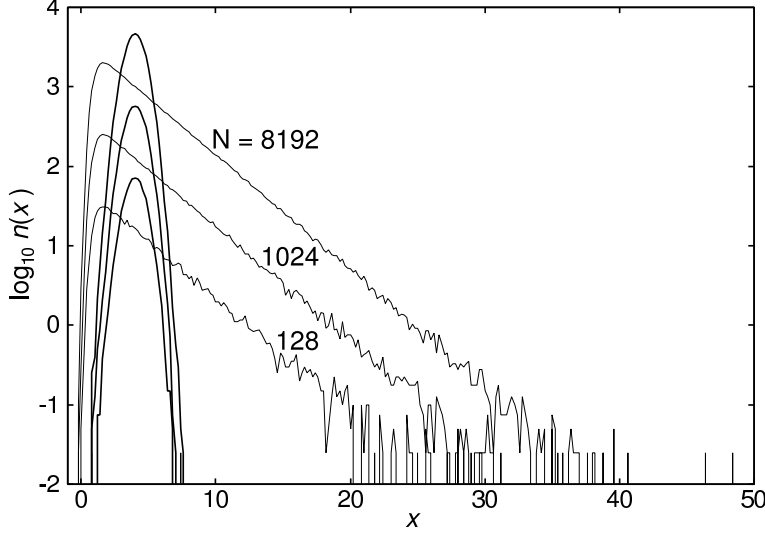


Fig. 12. Semilog plot of the distribution function  $n(x)$  of molecular distance for  $N = 128, 1024$  and  $N = 8192$ .  $\omega = 8, E_{\text{tot}} = 1.0$ .  $n(x)$  is normalized as  $\int n(x) dx = N$ . The initial distribution ( $t = 0$ ) and the distribution at  $t = 200$  are compared. At  $t = 0$ , the distribution is gaussian with the center on  $x = 4$ . The distribution at  $t = 200$  is almost final one and is well fitted to  $\sim e^{-x/x_0}$  with  $x_0 \sim 3$  for  $x \gg x_0$ . Each line was obtained from the average over 200 independent runs with nearly equilibrium initial states.

time scale of the present system:  $t_{\text{vib}} = 1/f_{\text{vib}} \approx 0.39$ . (The second peak is its harmonics at  $f = 2f_{\text{vib}}$ .)

The next small time scale (apart from the time scale of the inter-molecular potential:  $t_{\text{unit}} = r_0\sqrt{M/\phi_0} = 1$ ) is the mean free time (collision time):  $t_{\text{col}} \equiv L/\bar{v} \approx 4.9$ , where the molecular distance is  $L = 4$  and the average velocity of the molecule is  $\bar{v} \approx 0.82$  because the average translational energy is  $M\bar{v}^2/2 = K_{\text{tr}} \approx 1/3$ . Corresponding to this time scale, a mild hump around  $f_{\text{col}} \equiv 1/t_{\text{col}} \approx 0.21$  can be seen in the PSD of  $K_{\text{tr}}$ .

We have employed the initial states in which the positions  $q_i$  ( $i = 1, 2, \dots, N$ ) of molecules are distributed with Gaussian distribution with a small width around the equilibrium position as in (20). The distribution function  $n(x)$  of the molecular distance  $x = p_{i+1} - q_i$  is expected to tend to exponential:  $n(x) \sim e^{-x/x_0}$  for large  $x$  after a relatively short time which is long enough in comparison to  $t_{\text{col}}$ . This is because the molecular interaction is short range repulsive and each molecule occupies its position on a line independently. That is confirmed by semilog plot of  $n(x)$  for  $N = 128, 1024$  and  $N = 8182$  in Figure 12. The initial gaussian distribution with the center  $x = L$  tends to exponential with the average value  $x_0 \approx 3$  as can be explained in terms of the average distance  $L = 4$  and the scale of the repulsive potential  $r_0 = 1$  which yields  $x_0 \sim L - r_0 = 3$ .

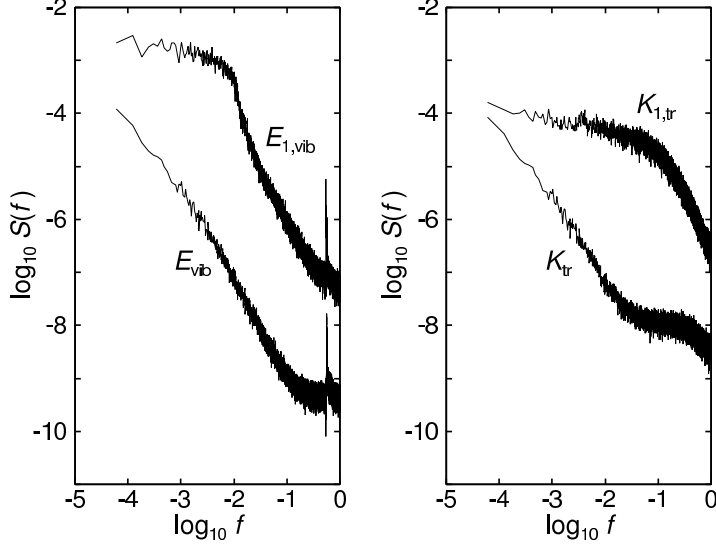


Fig. 13. The same as Fig. 11 but with a shorter observation time:  $t_{\text{obs}} = 1.6 \times 10^4$ .  $\Delta t = 0.5$  and  $N_{\text{dat}} = 2^{15}$ . The spectra of  $E_{\text{vib}}$  and  $K_{\text{vib}}$  is not yet saturated and look power-law like, while the spectra for the single molecule ( $E_{1,\text{vib}}$  and  $K_{1,\text{vib}}$ ) are nearly flat in a low frequency range.

The spectra of  $E_{\text{vib}}$  and  $K_{\text{tr}}$  are flat at frequencies lower than a certain frequency at the “shoulder” which we denote  $f_0$ . In Fig. 11(a), the shoulder frequency is  $f_0 \approx 10^{-5}$ . To observe the saturated spectrum (the spectrum which is white at low frequencies) one needs to observe the system for a time interval at least  $t_0 \equiv 1/f_0 \approx 10^5$ . In other words,  $t_0$  is a typical time scale after which the system loses the memory of the initial state. It should be pointed out that this long time scale characterizes the system in thermal equilibrium and does not depend on the specified initial state if chosen as an equilibrium one. To confirm it, we performed the simulation starting from the final state at  $t = t_{\text{obs}}$  of each run in (a) of Fig. 11 and continued the simulation for another time interval  $t_{\text{obs}}$ . The power spectra thus obtained were shown in (b) of Fig. 11, which is very similar to those in (a).

We have defined  $\bar{\tau}_{\text{cor}}$  as a characteristic time scale of the system, which is  $\bar{\tau}_{\text{cor}} \approx 1.1 \times 10^3$  in the case of  $N = 128$ ,  $\omega = 16$  (see Fig. 9). If the correlation function is pure exponential (Debye-type relaxation) as  $G(\tau) \sim e^{-2\pi f_c \tau}$ , the corresponding PSD is Lorentzian given by  $S(f) \sim 1/[1 + (f/f_c)^2]$  from the Wiener-Khinchin theorem and  $S(f)$  is flat at low frequencies  $f \lesssim f_c$ , i.e.  $f_c$  is the shoulder frequency. If our  $G(\tau)$  were exponential, this frequency should relate to the correlation time  $\tau_{\text{cor}}$  defined by (29) as  $f_c = \ln 2/2\pi\tau_{\text{col}} \sim \ln 2/2\pi\bar{\tau}_{\text{col}} \approx 1.0 \times 10^{-4}$ . As we have seen in the above, the shoulder frequency  $f_0$  is much smaller (at least more than one digit) than  $f_c$ , which means that decay of the correlation function is slower than exponential, i.e. the PSD function deviates from Lorentzian. (See below.)

The long time scale appears clearly when one observes the energy involved with

all molecules but not the energy of individual ones. The spectra of the vibrational and translational energies of molecule 1 ( $E_{1,\text{vib}} \equiv \pi_1^2/2M + M\omega^2\xi_1^2/2$  and  $K_{1,\text{tr}} \equiv p_1^2/2M$ ) are also presented in Fig. 11. The shoulder frequencies in these spectra are much higher (order of three or four digits) than in the spectra of  $E_{\text{vib}}$  and  $K_{\text{vib}}$ , implying that each molecule loses its initial memory much faster than the total system. Similar results for the energy power spectra of the total system and the individual molecules have been obtained from MD simulations of liquid water [9].

The long time scale is often related to the power law of PSD as  $\sim 1/f^\alpha$  with  $0 < \alpha < 2$  over a wide range of frequency. It should be noted, however, that the spectrum sometimes appears to be  $1/f^\alpha$ -like when the observation time  $t_{\text{obs}}$  is not long enough. Power spectra obtained from the same simulations as in Fig 11 but with a shorter observation time:  $t_{\text{obs}} \approx 1.6 \times 10^4$  and a longer sampling time  $\Delta t = 0.5$  are presented in Fig. 13 [29]. For energies of the single molecule, the power spectra are saturated, i.e. white at low frequencies, while the spectra of  $E_{\text{vib}}$  and  $K_{\text{tr}}$  look like  $\sim 1/f^\alpha$  with  $\alpha$  being  $1.4 \sim 1.5$  over a low frequency range of about two digits and no shoulders are observed because the lowest frequency  $1/t_{\text{obs}}$  is higher than  $f_0$ . As mentioned above, these spectra deviate from the Lorentzian form in which  $\alpha = 2$  should be expected for  $f \gtrsim f_0$ . The value of  $\alpha$  smaller than two might be attributed to the heterogeneity, i.e. the system is more complex because of the internal degrees of freedom. In fact, MD simulations of much more complex systems [9] (three-dimensional liquid water, alcohol and argon cluster) yielded power spectra whose exponent  $\alpha$  of the power-law decaying part is smaller than the present value.

### 3.5 Relaxation from nonequilibrium initial states

In deriving the time scale in Eq. (6) from the Landau-Teller approximation, a nonequilibrium initial state is assumed and the relaxation time toward equilibrium is estimated. Here we perform simulations based on this idea and initially prepare the system with different temperatures for subsystems of the translational and vibrational motion. We set the energies of subsystems as  $K_{\text{tr},0} = 0.2$  and  $E_{\text{vib},0} \equiv K_{\text{vib},0} + V_{\text{vib},0} = 0.8$  corresponding to the initial temperatures  $kT_{\text{tr},0} = 2K_{\text{tr},0} = 0.4$  and  $kT_{\text{vib},0} = E_{\text{vib},0} = 0.8$ . In Fig. 14, the temporal variation of the quantity  $E_{\text{vib}} - 2K_{\text{tr}} = k(T_{\text{vib}} - T_{\text{tr}})$  is presented for various values of  $\omega$ , which shows how the temperature difference of two subsystems tends to zero and the thermal equilibrium is realized.

If the temperature difference  $\Delta T \equiv T_{\text{vib}} - T_{\text{tr}}$  decays as

$$\frac{d}{dt}\Delta T(t) = -\frac{\Delta T(t)}{\tau_1}, \quad (35)$$

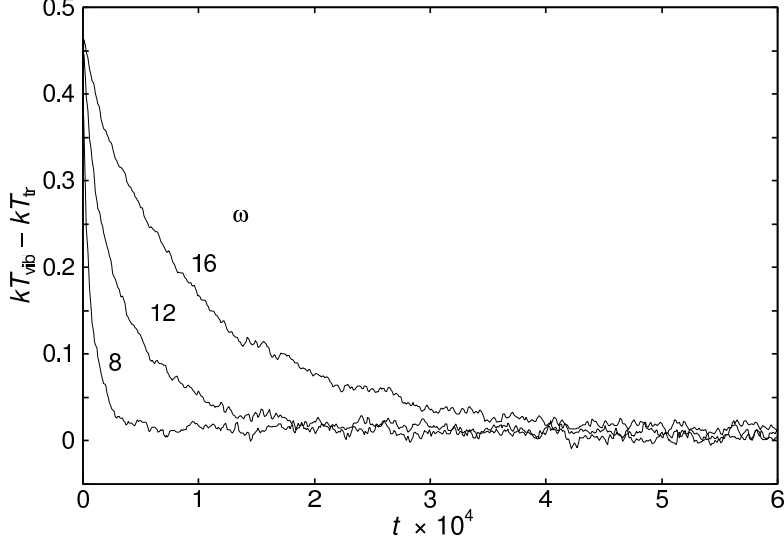


Fig. 14. Temperature difference between the vibrational and translational motion.  $N = 128$ . Temporal variation of  $k\Delta T \equiv kT_{\text{vib}} - kT_{\text{tr}} \equiv E_{\text{vib}} - 2K_{\text{tr}}$  is plotted for  $\omega = 8, 12, 16$ . Each line was obtained from the average over 200 independent runs with different initial states satisfying the condition  $E_{\text{tot},0} = 1$ ,  $K_{\text{vib},0} = V_{\text{vib},0} = 0.4$ ,  $K_{\text{tr},0} = 0.2$ ,  $V_{\text{int},0} \approx 0$  so that the initial temperature is  $kT_{\text{vib},0} = 0.8$ ,  $kT_{\text{tr},0} = 0.4$ . The plotted point at the time  $t$  represents the average over the time interval  $[t-100, t+100]$ . The sampling interval of plotting is  $\Delta t = 100$ .

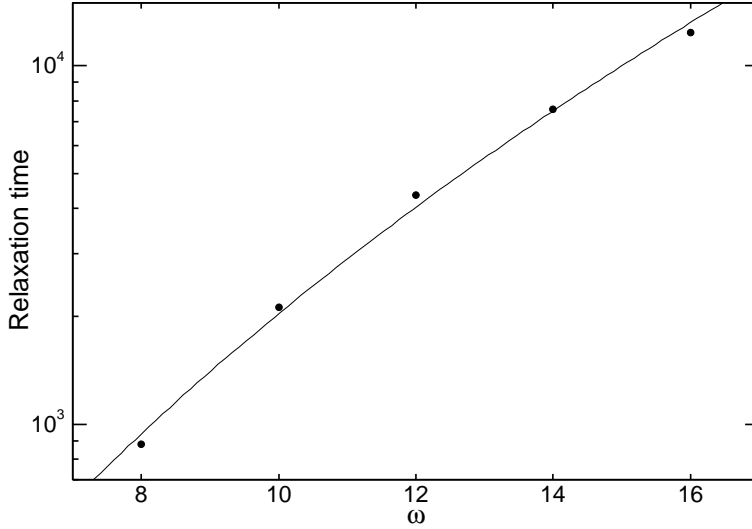


Fig. 15. Semilog plot of  $\omega$ -dependence of the relaxation time  $\tau_1$  defined in Eq. (35).  $N = 128$ ,  $E_{\text{tot}} = 1.0$ . The same initial condition as in Fig. 14. The guide line is  $A_1 \exp[B_1 \omega^{0.4}]$  with  $A_1 = 0.204$  and  $B_1 = 3.601$ .

the relaxation time  $\tau_1$  derived from the Landau-Teller approximation depends on  $\omega$  and  $T_{\text{tr}}$ , and its main  $\omega$ -dependence is obtained as  $\tau_1 = C \exp[B\omega^\alpha]$ , where  $C$  still depends on  $\omega$  weakly and on  $T_{\text{tr}}$  [17]. If  $T_{\text{tr}}$ -dependence of  $C$  could be ignored, the lines in Fig. 14 should be fitted to  $k\Delta T(t) = k\Delta T(0)e^{-t/\tau_1}$

with  $k\Delta T(0) = 0.4$ . In fact, these lines exhibit some oscillations as a function of the time  $t$ , even though each line has been obtained from the average over the time interval  $[100 - t, t + 100]$  and from the average over 200 independent runs. Especially the lines (for larger values of  $\omega$ ) starting from 0.4 do not decrease in the beginning but increase steeply (up to  $\approx 0.47$  for  $\omega = 16$ ) [31]. Hence, the fitting to the exponentially decreasing function is very rough. We, however, estimated the relaxation time  $\tau_1$  using the fitting function  $0.4 e^{-t/\tau_1}$ . The  $\omega$ -dependence of  $\tau_1$  is given in Fig. 15 and the guide line is obtained from  $\tau_1 = A_1 \exp[B_1 \omega^{0.4}]$  with  $A_1 = 0.240$  and  $B_1 = 3.601$ . In comparison to the correlation time (see Fig. 9), data points of  $\tau_1$  appreciably deviate from the fitting line. The main reason might be the temperature dependence of  $\tau_1$  in Eq. (35) which has been ignored. The correlation time is estimated in thermal equilibrium, while the relaxation time here is defined in the nonequilibrium state, and the smaller the temperature difference, the better the approximation [32].

Next we compare the relaxation time  $\tau_1$  (the time scale of energy exchange between the vibrational and the translational motion) and another time scale: the time scale of energy relaxation *within* the vibrational degrees of freedom. we carried out a simulation starting from a nonequilibrium vibrational state, i.e. the initial state is such that the vibrational motion of subsystems I (composed of the first  $N/2$  molecules) and II (composed of the rest  $N/2$  molecules) are in different thermal equilibrium, while the translational motion is in another thermal equilibrium state as a whole. The initial values of vibrational energies (per molecule)  $E_{I,\text{vib}}$ ,  $E_{II,\text{vib}}$  of subsystems I and II were chosen as  $E_{I,\text{vib},0} = 2E_{\text{vib},0}$  and  $E_{II,\text{vib},0} = 0$ , respectively.

Fig. 16 shows the case for  $N = 256$ ,  $\omega = 16$  and for the initial condition  $E_{\text{vib},0} = 0.8$  and  $K_{\text{tr},0} = 0.2$ , where plotted points were obtained by the average over 20 different runs. The temperature difference defined by  $k\Delta T \equiv E_{\text{vib}} - 2K_{\text{tr}}$ , starting from  $k\Delta T_0 = 0.4$ , decays monotonically, while the temperature difference  $k\Delta T_{\text{vib}} \equiv E_{I,\text{vib}} - E_{II,\text{vib}}$  exhibits a damping oscillation. For a fixed value of  $\omega$ , the first zero-crossing time of  $k\Delta T_{\text{vib}}$  increases linearly with  $N$ , and the amplitude of the damping oscillation, i.e. the most negative value of  $k\Delta T_{\text{vib}}$  turned out to decrease with increasing  $N$ . On the other hand, for a fixed value of  $N$ , the first zero-crossing time of  $k\Delta T_{\text{vib}}$  increases weakly with increasing  $\omega$  but  $\tau_1$ , i.e. the time scale of  $k\Delta T$  increases much strongly ( $\sim \exp^{B\omega^{0.4}}$ ). Thus, for sufficiently large values of both  $N$  and  $\omega$ , the time scale of energy exchange between the translational and vibrational motion is much larger than that of energy relaxation within the vibrational system, which can actually be seen in Fig. 16.

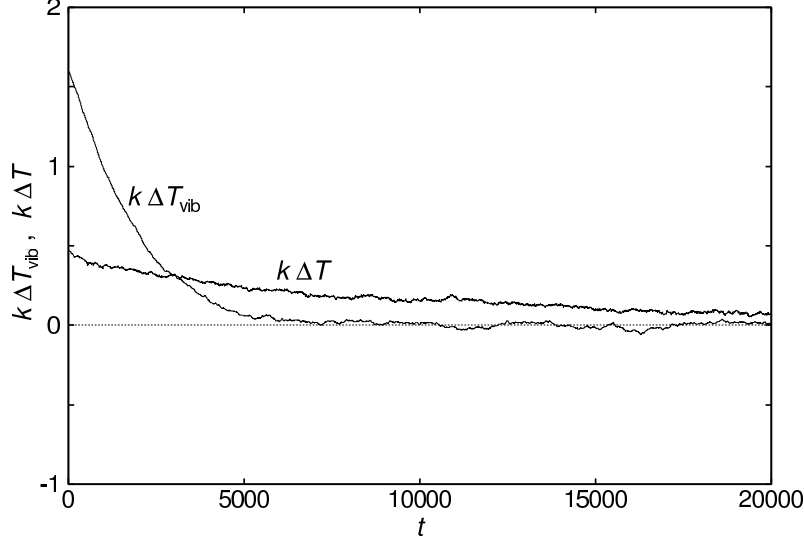


Fig. 16. Temporal variation of the quantities  $k\Delta T \equiv E_{\text{vib}} - 2K_{\text{tr}}$  and  $k\Delta T_{\text{vib}} \equiv E_{\text{I,vib}} - E_{\text{II,vib}}$ , where the suffixes I and II indicate the subsystems composed of the first  $N/2$  and the rest  $N/2$  molecules, respectively. Initial condition:  $E_{\text{tot},0} = 1$ ,  $E_{\text{vib},0} = 0.8$ ,  $K_{\text{tr},0} = 0.2$ ,  $V_{\text{int},0} \approx 0$ . The vibrational energy is distributed only to the subsystem I so that  $K_{\text{I,vib},0} = V_{\text{I,vib},0} = 0.8$ , and  $K_{\text{II,vib},0} = V_{\text{II,vib},0} = 0$ . Each line was obtained from the average over 20 independent runs satisfying the same initial condition.  $N = 256$ ,  $\omega = 16$ . The sampling interval of plotting is  $\Delta t = 5$ .

### 3.6 Effect of deviation from the complete resonance

As mentioned already, the exponent  $\alpha$  in Eq. (4) generally depends on the number  $N$  of degrees of freedom, and the long time scale might not be realized for large  $N$  except when all  $\omega_i$ 's are equal to each other. Also in the Landau-Teller approximation, the binary collisions are such that the vibrational frequency of each molecule is identical. Hence it is interesting to investigate whether the condition of the complete resonance is essential for the long time scale in the system with many degrees of freedom.

We have chosen homogeneous random numbers  $(\omega_1, \dots, \omega_N)$  in the interval  $[\omega - \Delta\omega/2, \omega + \Delta\omega/2]$ , whose average is  $\omega$ . Fig. 17 shows  $\Delta\omega$ -dependence of the correlation time for  $N = 128$ ,  $E_{\text{tot}} = 1$ ,  $\omega = 8$ . The correlation time decreased with increasing  $\Delta\omega$  monotonically, but its  $\Delta\omega$ -dependence is rather complicated, which we have not yet investigated.

By assuming a fixed small value for  $\Delta\omega$  as  $\Delta\omega = 0.1$ , we obtained the  $\omega$ -dependence of the correlation time as in Fig. 18. The present result shows that the condition of complete resonance:  $\omega_1 = \dots = \omega_N$  is not essential for the long time scale because the correlation time increases with  $\omega$  in the same way as in  $\Delta\omega = 0$  for a finite (but small) value of  $\Delta\omega$ .

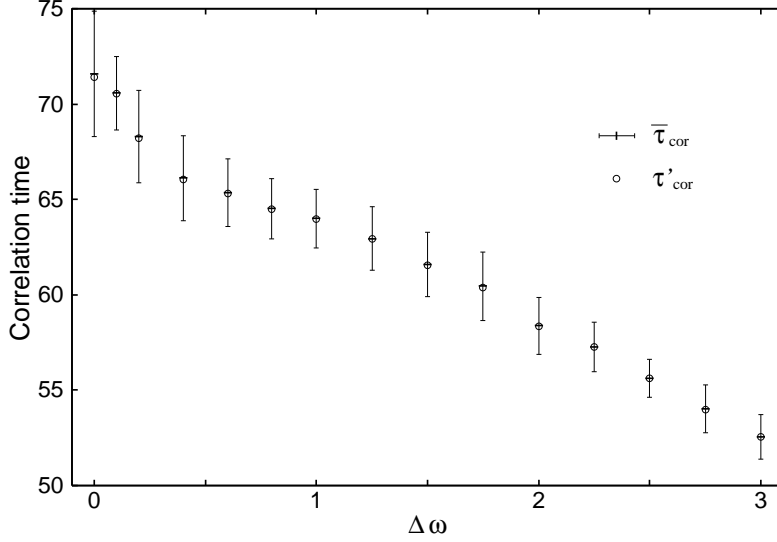


Fig. 17.  $\Delta\omega$ -dependence of the averaged correlation time  $\bar{\tau}_{\text{cor}}$ .  $N = 128$ ,  $E_{\text{tot}} = 1.0$ . The vibrational frequencies of molecules ( $\omega_1, \dots, \omega_N$ ) are generated from homogeneous random numbers with the width  $\Delta\omega$  and a fixed average value  $\omega = 8$ .  $\bar{\tau}_{\text{cor}}$  is obtained from the average over 40 independent runs with nearly equilibrium initial states. Error bars indicate  $\bar{\tau}_{\text{cor}} \pm \sigma$ , where  $\sigma$  is the standard deviation. The points of  $\Delta\omega = 0$  correspond to those of  $N = 128$  in Fig. 9 but obtained from 40 runs.

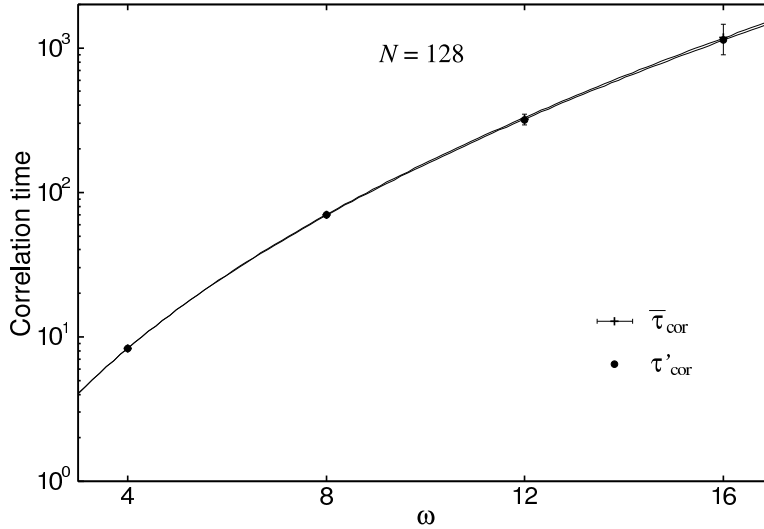


Fig. 18. Semilog plot of  $\omega$ -dependence of  $\bar{\tau}_{\text{cor}}$  for a fixed value of  $\Delta\omega = 0.1$ .  $N = 128$ ,  $E_{\text{tot}} = 1.0$ . The average is taken over 40 independent runs with nearly equilibrium initial states and error bars express  $\pm\sigma$ . The guide line corresponds to  $\bar{\tau}_{\text{cor}} = A \exp[B \times \omega^{0.4}]$  with  $A = 0.0106$ ,  $B = 3.83$ .

#### 4 Conclusions and Discussions

In conclusion, we estimated the correlation time  $\tau_{\text{cor}}$  of the vibrational energy which is defined in thermal equilibrium. The present simulations yielded the

time scale which indeed remains finite in the large  $N$  limit and grows as  $\sim \exp B\omega^{0.4}$  in good agreement with that obtained from the Landau-Teller approximation. The condition of the complete resonance assumed both in the mathematical theorem based on the perturbation method and in the Landau-Teller approximation is not essential for the long time scale because a slight deviation from the complete resonance did not change the  $\omega$ -dependence of the time scale.

Concerning the system size dependence, we found that the correlation time  $\tau_{\text{cor}}(N)$  decreased in the beginning but tends to a finite value with increasing  $N$  for a fixed value of the molecular density. If the molecular density  $\rho \equiv N/L_{\text{tot}} = 1/L$  ( $L_{\text{tot}}$  is the length of the system) is small enough so that three-molecule collisions can be neglected, then one can expect  $\tau_{\text{cor}}(N)$  being constant (for a fixed value of  $\rho$ ). In other words, the system size dependence of the time scale is regarded as arising from multi-molecular collisions. Then a natural question arises: Does the long time scale in the thermodynamic limit remains for high density case? The present paper does not answer this question.

The present study was done for a one-dimensional gas. To what extent does the one-dimensional scenario work in higher dimensional gases? On this issue, we note the case of FPU-type systems (as a model of lattice vibrations) [26]: The long time scale remains in a one-dimensional chain but disappeared in a two-dimensional lattice, which suggests the difficulty in predicting a correct answer for the gas model too. No systematic study of the size dependence has been reported for higher-dimensional systems including solids and liquid. Nevertheless, our feeling is that, as suggested in [9], if the system is heterogeneous (i.e. composed of subsystems with well separated time scales), the basic idea of Boltzmann and Jeans might be still usable and so the slow relaxation might be realizable in the thermodynamic limit for the high-dimensional gases as well and even for more general systems covering liquid and solid.

The power spectra of the energy fluctuations obtained in the present simulations are  $1/f^\alpha$ -like with  $\alpha$  around  $1.4 \sim 1.5$  in a range of low frequencies. In “real”  $1/f$  fluctuations (or noise) observed in, say, the electrical resistance of condensed matter systems,  $\alpha$  is nearly constant and very close to one over a wide range of frequencies. Typical upper limits of the power-law decaying range are from 100 to  $10^4$ Hz, and a typical lower limit is  $10^{-2}$ Hz. (In some case the lower limit has been reported to be extended down to  $10^{-7}$ Hz without observing the shoulder frequency.) [22] Until now, such beautiful  $1/f$  fluctuations have never been reproduced from any Hamiltonian systems with many degrees of freedom. In case of one-dimensional FPU  $\beta$ -model, it was found [23], for large  $N$ , that the shoulder frequency  $f_0$  of the lowest mode energy spectrum decreases with increasing  $N$ , while the spectrum is close to Lorentzian:  $\alpha \approx 2$  in a frequency range  $f \gtrsim f_0$ . In other words, the energy fluctuations of the

FPU  $\beta$ -model cannot be said as  $1/f$ -type even if the time scale  $\sim 1/f_0$  might be long. In contrast, the spectra for diatomic gas obtained here deviate from Lorentzian and have an exponent  $\alpha$  smaller than two.

Brillouin scattering experiments on quartz [24] showed that phonon number fluctuations (energy fluctuations of each normal mode) exhibit  $1/f^\alpha$  spectra over a frequency range from  $10^{-4}$  to  $10^{-1}$  Hz. In similar experiments on liquid water [25],  $1/f^\alpha$  spectra were also observed, in which the frequency range is even wider:  $10^{-4}$  to  $10^1$  Hz. In both cases,  $\alpha$  is close to one and no shoulder appears during the observation time which is of orders of hours ( $\sim 10^4$  s). As stated above, one-dimensional FPU models are unsatisfactory to explain such  $1/f$  noise. On the other hand, modified FPU models having internal degrees of freedom seem to be a better candidate. Actually, the analysis of a modified one-dimensional FPU model [6] is suggestive, in which the long time scale was proved to remain in the thermodynamic limit. At this stage, we think much of investigation into the power spectra of such systems to know whether the power-law decaying range could be wide enough in the thermodynamic limit and, more importantly, whether  $\alpha$  could approach one owing to the internal degrees of freedom.

## Acknowledgments

We are grateful to T. Kimura who collaborated with us at the early stage of this work.

## References

- [1] L. Boltzmann, *Nature* **51** (1895) 413.
- [2] J. H. Jeans, *Philos. Mag.* **6** (1903) 279.
- [3] G. Benettin, L. Galgani and A. Giorgilli, *Phys. Lett. A* **120** (1987) 23.
- [4] G. Benettin, L. Galgani and A. Giorgilli, *Commun. Math. Phys.* **113** (1987) 87.
- [5] G. Benettin, L. Galgani and A. Giorgilli, *Commun. Math. Phys.* **121** (1989) 557.
- [6] L. Galgani, A. Giorgilli, A. Martinoli and S. Vanzini, *Physica D* **59** (1992) 334.
- [7] M. Sasai, I. Ohmine and R. Ramaswamy, *J. Chem. Phys.* **96** (1992) 3045.
- [8] A. Ishijima, H. Kojima, T. Funatsu, M. Tokunaga, H. Higuchi, H. Tanaka and T. Yanagida, *Cell* **92** (1998) 161.
- [9] A. Shudo and S. Saito, *Adv. Chem. Phys. B* **130** (2005) 375.
- [10] N. Nakagawa and K. Kaneko, *Phys. Rev. E* **64** (2001) 055205(R).

- [11] N. N. Nekhoroshev, Usp. Mat. Nauk **32** (1977). [Russ. Math. Surv. **32** (1977) 1.]
- [12] E. Fermi, J. Pasta and S. Ulam, Los Alamos Report No. LA-1940 (1955), in *Collected Papers of Enrico Fermi*, vol. II (Univ. Chicago Press, 1965) p. 978.
- [13] G. Benettin, Proc. Int. School of Phys. ENRICO FERMI, Course XCVII, ed. G. Ciccotti and W. G. Hoover (1986) p. 15.
- [14] L. Berchialla, A. Giorgilli and S. Paleari, Phys. Lett. A **321** (2004) 167.
- [15] G. Benettin, Chaos **15** (2005) 015108.
- [16] G. Benettin, Prog. Theor. Phys. Suppl. No. 116 (1994) 207.
- [17] G. Benettin, P. Hjorth, and P. Sempio, J. Stat. Phys. **94** (1999) 871.
- [18] L. Landau and E. Teller, Phys. Z. Sowjet. **10** (1936) 34, in *Collected Papers of L. D. Landau*, ed. D. Ter Haar (Pergamon Press, 1965) p. 147.
- [19] D. Rapp, J. Chem. Phys. **32** (1960) 735.
- [20] H. Yoshida, Phys. Lett. A **150** (1990) 262.
- [21] W. H. Press, S. A. Teukolsky, W. T. Vetterling and B. P. Flannery, Numerical Recipes in C++, 2nd ed. pp. 205. (Cambridge Univ. Press, Cambridge, UK. 2002)
- [22] P. Dutta and P. M. Horn, Rev. Mod. Phys. **53** (1981) 497.
- [23] H. Kawamura, N. Fuchikami, D. Choi and S. Ishioka, Jpn. J. Appl. Phys. **35** (1996) 2387.
- [24] T. Musha, G. Borbely and M. Shoji, Phys. Rev. Lett. **64** (1990) 2394.
- [25] T. Musha and G. Borbely, Jpn. J. Appl. Phys. **31** (1992) L370.
- [26] In fact, the numerical simulation of the FPU  $\beta$ -model showed the long time scale as  $\sim \exp[(1/\varepsilon)^{0.25}]$  (here  $\varepsilon$  is the total energy divided by  $N$ ) in the limit  $N \rightarrow \infty$  [14], while in the FPU  $\alpha$ -model [6] and also in a two-dimensional FPU lattice [15], the non-ergodic behavior disappeared.
- [27] The system here is the same as that employed in [3] except the boundary condition and maybe the details of the initial condition.
- [28] Even though random numbers are generated such that their probability distribution function  $P(x)$  satisfies  $\int xP(x)dx = 0$ , this does not mean that the average value of these numbers actually vanishes.
- [29] The peaks at  $f = f_{\text{vib}} - 1/\Delta t \approx 0.55$  in the spectra of  $E_{\text{vib}}$  and  $E_{1,\text{vib}}$  are an artifact arising from the aliasing effect [21].
- [30] Note that the parameters  $(A, B)$  and  $(A', B')$  do not need to coincide because those parameters depend on the initial state of each run. Here the correlation times were obtained from 20 random initial conditions and the average values  $\bar{\tau}_{\text{cor}}$  and  $\tau'_{\text{cor}}$  are defined in different ways.

- [31] It turned out that this increase corresponds to the situation that the initial energy transfer occurs mainly from  $K_{\text{tr}}$  to  $V_{\text{int}}$ , while  $E_{\text{vib}}$  stays almost constant.
- [32] Remembering the non-exponential decay of  $G(\tau)$ , we like to mention another possibility: The time-dependence of the temperature difference  $\Delta T$  might deviate from pure exponential.